

The roles of quantum correlations in quantum cloning

Jun Zhang, Shao-xiong Wu, and Chang-shui Yu^a

School of Physics and Optoelectronic Technology, Dalian University of Technology, Dalian 116024, China

Received: date / Revised version: date

Abstract. In this paper, we study the entanglement and quantum discord of the output modes in the unified $1 \rightarrow 2$ state-dependent cloning and probabilistic quantum cloning. The tripartite entanglement among the output modes and the quantum cloning machine is also considered. We find that the roles of the quantum correlations including the bipartite and tripartite entanglement and quantum discord strongly depend on the quantum cloning machines as well as the cloned state. In particular, it is found that this quantum cloning scheme can be realizable even without any quantum correlation.

PACS. 03.67.Mn 03.67.—a 03.65.Ud

1 Introduction

In recent years, quantum information theory has been developed greatly, whilst a lot of quantum information processing tasks have been invented and realized such as quantum teleportation [1], quantum entanglement purification [2,3], quantum key distribution [4,5] and so on [6,7,8]. In particular, quantum key distribution, compared with the classical cryptography, has the distinguished security which is guaranteed by the fundamental principle, i.e., 'Quantum No-Cloning Theorem' (QNCT) [9].

QNCT states that an unknown quantum state cannot be cloned (perfectly copied) [9], however, the approximate cloning can always be realized based on some proper quantum schemes (quantum cloning machines). The approximate cloning usually includes two types: one is the probabilistic quantum cloning by which a set of linearly independent states can be faithfully copied with a certain success probability [10], and the other is the unfaithful quantum cloning by which the output state is not a faithful copy of the input state [11,12]. Of course, the fidelity of the output state in the unfaithful quantum cloning could depends on the input state. The approximate quantum cloning has attracted widely interests and there appears many interesting quantum cloning machines such as the phase-covariant quantum cloning [13,14,15,16,17,18], the optimal phase-independent cloning [20], entanglement of quantum cloning [21,22,23,24], the orthogonal qubit quantum cloning [25], the optimal nonorthogonal quantum cloning [26] and so on [6,7]. Among the various quantum clonings, Wang *et al.* have proposed a unified way to construct general asymmetric universal quantum cloning machine [27]. In particular, the Buzek-Hillery quantum cloning machine (BHC) has shown to be a universal one because it achieves equal fidelity $\frac{5}{6}$ for any quantum state

[28]. However, in the BHC including many unfaithful cloning schemes, the two output modes are usually correlated with each other. Compared with the separable output modes in the ideal quantum cloning, intuitively it seems that the output correlated modes could play the negative role in the cloning. That is, the success probability or the fidelity of the output state could be reduced by the existing correlation. Such an intuition is also supported by a recent job which shows, as a general viewpoint for the imperfect cloning, that the amount of correlation between the original and the cloned copy in the output will prevent from copying the information of the original state in the blank state [29]. On the contrary, some other results show that in the probabilistic pure state cloning there is no entanglement, but quantum correlation is always present [30]. And for a certain class of optimal cloners, in order to reach higher fidelities, entanglement is needed [31]. So what are the roles of quantum correlations in the quantum cloning?

In this paper, we attempt to show that the roles of quantum correlations including the concurrence, 3-tangle and quantum discord depend on the quantum cloning scheme and the cloned states. Or from a general point of view, there does not exist one-to-one map between quantum cloning and quantum correlation as well as quantum entanglement. In order to support our points, we consider the optimal nonorthogonal quantum cloning machine which unifies the $1 \rightarrow 2$ state-dependent cloning and probabilistic quantum cloning [26]. In this scheme, we find that given two states to be cloned and an expected success probability (fidelity), the same fidelity (success probability) could correspond to different quantum correlations. On the contrary, a fixed quantum correlation could also corresponds to different fidelities or success probabilities. Thus the most distinct advantage is that for the fixed fidelity or success probability, one will has diverse ways to control the cloning procedure with various quantum

^a quaninformation@sina.com; ycs@dlut.edu.cn

correlations taken into account, or one will always find a way to implement the cloning with the less cost, since the quantum correlations could be some important physical resources. Finally, we also find that if there is no quantum correlation in the scheme, the quantum cloning can also be realized.

This paper is organized as follows. In Sec. II, we give a brief introduction of the unified $1 \rightarrow 2$ quantum cloning. In Sec. III, we study how the success probability and the fidelity are influenced by the bipartite and tripartite entanglement as well as quantum discord. In Sec. IV, we present a successful cloning without any quantum correlation. Finally, the conclusion is drawn.

2 Unified $1 \rightarrow 2$ quantum cloning

To begin with, let's give a brief introduction of the transformations in the unified $1 \rightarrow 2$ state-dependent cloning and probabilistic quantum cloning. The action of this quantum cloning is given by the transformations [26]

$$\begin{aligned} |0\rangle|0\rangle|0\rangle_p &\rightarrow [A|00\rangle + B(|01\rangle + |10\rangle) + C|11\rangle]|0\rangle_p \\ &\quad + D|00\rangle|1\rangle_p, \\ |1\rangle|0\rangle|0\rangle_p &\rightarrow [A|11\rangle + B(|01\rangle + |10\rangle) + C|00\rangle]|0\rangle_p \\ &\quad + D|00\rangle|1\rangle_p, \end{aligned} \quad (1)$$

where A, B, C, D are real constants for simplicity and satisfy the orthonormal condition:

$$A^2 + 2B^2 + C^2 + D^2 = 1, \quad (2)$$

$$2AC + 2B^2 + D^2 = 0. \quad (3)$$

with the subscript 'p' marking the probing state. Now, suppose we clone a set of two nonorthogonal quantum states in the following form

$$|\chi_1\rangle = \cos\theta|0\rangle + \sin\theta|1\rangle, \quad (4)$$

$$|\chi_2\rangle = \sin\theta|0\rangle + \cos\theta|1\rangle. \quad (5)$$

where $\theta \in [0, \pi/4]$, with their overlap given by

$$s = \langle\chi_1|\chi_2\rangle = \sin 2\theta. \quad (6)$$

After the cloning transformations, the output states corresponding to the two nonorthogonal quantum states are given, respectively, by

$$\begin{aligned} |\chi_1\rangle^{(out)} &= [(A \cos\theta + C \sin\theta)|00\rangle \\ &\quad + B(\cos\theta + \sin\theta)(|01\rangle + |10\rangle) \\ &\quad + (C \cos\theta + A \sin\theta)|11\rangle]|0\rangle_p \\ &\quad + D(\cos\theta + \sin\theta)|00\rangle|1\rangle_p \\ &= \sqrt{\gamma}|X_1\rangle|0\rangle_p + \sqrt{1-\gamma}|00\rangle|1\rangle_p, \end{aligned} \quad (7)$$

$$\begin{aligned} |\chi_2\rangle^{(out)} &= [(A \sin\theta + C \cos\theta)|00\rangle \\ &\quad + B(\sin\theta + \cos\theta)(|01\rangle + |10\rangle) \\ &\quad + (C \sin\theta + A \cos\theta)|11\rangle]|0\rangle_p \\ &\quad + D(\sin\theta + \cos\theta)|00\rangle|1\rangle_p \\ &= \sqrt{\gamma}|X_2\rangle|0\rangle_p + \sqrt{1-\gamma}|00\rangle|1\rangle_p, \end{aligned} \quad (8)$$

where $\sqrt{\gamma}|X_i\rangle = \langle 0_p|\chi_i\rangle^{(out)}$, γ is the normalization of $\langle 0_p|\chi_i\rangle^{(out)}$ denoting the probability with which one will obtains the $\langle 0_p|$ if one measures the probing qubit. Note that γ is a function of A, B, C, D and θ . If the probing state $|0\rangle_p$ is detected by some measurement, $|\chi_i\rangle^{(out)}$ will collapses to the state $|X_i\rangle$ with the probability γ , which means that this cloning is not only probabilistic but also state-dependent and the fidelity is given by the overlap between the output state $\text{Tr}_\alpha \{|X_i\rangle\langle X_i|\}$ and the input state $|\chi_i\rangle$, i.e.,

$$f = \frac{1}{4\gamma}[(A - 2B - C)(A + C) \cos 4\theta + 2BC + C^2 + 3A^2 + 4(A + B)(B + C) \sin 2\theta + 2AB + 4B^2], \quad (9)$$

where α in the subscript denotes trace over either subsystem. A simple calculation will shows that this cloning is symmetric because the fidelity f pertains to both $|X_1\rangle$ and $|X_2\rangle$. In addition, this fidelity f is not an optimal one. The optimal case will be discussed in the latter section. If $|1\rangle_p$ is obtained for some measurement, it means that the cloning fails. If the success probability $\gamma = 1$, the cloning is called the state-dependent cloning (SDC), otherwise, the cloning is considered as a probabilistic one with the success probability denoted by $\gamma^{(PQC)} = \gamma$.

3 Quantum correlation in the quantum cloning

3.1 Quantum entanglement

In order to find the relation between the quantum entanglement and the fidelity, we have to first deal with the fidelity given by Eq. (9). Consider Eqs.(2,3,6,7,8), we can find that $D = \sqrt{\frac{1-\gamma}{1+s}}$ and the values of A and C are given by

$$\begin{cases} A_{1\pm} = \frac{1}{2} \left(\pm \sqrt{\frac{s+2\gamma-1}{1+s}} - 4B^2 + 1 \right), \\ C_{1\pm} = \frac{1}{2} \left(\pm \sqrt{\frac{s+2\gamma-1}{1+s}} - 4B^2 - 1 \right). \end{cases} \quad (10)$$

or

$$\begin{cases} A_{2\pm} = \frac{1}{2} \left(\mp \sqrt{\frac{s+2\gamma-1}{1+s}} - 4B^2 - 1 \right), \\ C_{2\pm} = \frac{1}{2} \left(\mp \sqrt{\frac{s+2\gamma-1}{1+s}} - 4B^2 + 1 \right). \end{cases} \quad (11)$$

We would like to emphasize $\gamma \geq \frac{1-s}{2}$ and $B \in \left[-\frac{\sqrt{1-2D^2}}{2}, \frac{\sqrt{1-2D^2}}{2}\right]$ due to the real A, C . This condition will be used throughout of this paper. Insert Eqs. (10,11) into Eq. (9), through a long and tedious procedure one will finds that the general (unoptimized) fidelity reads

$$f_{1\pm} = \frac{1}{2} \pm \frac{(1+s)[1 + (2B-1)s]}{2\gamma} \sqrt{\frac{s-1-4B^2(1+s)+2\gamma}{1+s}}. \quad (12)$$

or

$$f_{2\pm} = \frac{1}{2} \mp \frac{(1+s)[-1 + (2B+1)s]}{2\gamma} \sqrt{\frac{s-1-4B^2(1+s)+2\gamma}{1+s}}. \quad (13)$$

Since it is always implied that the maximal output fidelity is expected for any s , γ and B , one can find that such a partially optimal fidelity can be given by $f_p = \max\{f_{1\pm}, f_{2\pm}\}$. Thus for a pair of fixed input states (fixed s) and the expected success probability γ , f_p is a function of the parameter B , from which one can find out how to increase the fidelity f_p by adjusting B . In addition, it will be shown that the parameter B of the cloners is important for the connection with entanglement.

In the following, we will find out the amount of entanglement hidden in the two output modes. Due to the symmetry of the transformation given by Eq. (1), we will only consider the state $|\chi_1\rangle^{out}$. It can be easily shown that $|\chi_2\rangle^{out}$ has the same result which is not repeated. The state of the two output modes can be easily obtained from Eqs. (7,8), by tracing over the probing qubit p . So the reduced density matrix of the two output modes can be given in the following form:

$$\rho = \begin{pmatrix} a^2 + d^2 & ab & ab & ac \\ ab & b^2 & b^2 & bc \\ ab & b^2 & b^2 & bc \\ ac & bc & bc & c^2 \end{pmatrix}. \quad (14)$$

with

$$a = A \cos \theta + C \sin \theta, \quad (15)$$

$$b = B(\cos \theta + \sin \theta), \quad (16)$$

$$c = C \cos \theta + A \sin \theta, \quad (17)$$

$$d = D(\cos \theta + \sin \theta). \quad (18)$$

Note that A , B , C , D are determined by Eqs. (10,11). In order to quantify the entanglement in the state ρ , we would like to employ the concurrence as the entanglement measure which is defined for a density matrix ρ as [32]

$$C(\rho) = \max\{0, \sqrt{\lambda_1} - \sqrt{\lambda_2} - \sqrt{\lambda_3} - \sqrt{\lambda_4}\}, \quad (19)$$

where λ_i is the square root of the i th eigenvalue of the matrix $\rho \sigma_y \otimes \sigma_y \rho^* \sigma_y \otimes \sigma_y$ in decreasing order with σ_y denoting the Pauli matrix. Substitute the density matrix ρ into Eq. (19), one will obtain that

$$\lambda_{1,2} = 0, \lambda_{3,4} = \alpha \pm \beta. \quad (20)$$

with

$$\alpha = 2(b^2 - ac)^2 + c^2 d^2, \quad (21)$$

$$\beta = 2|b^2 - ac| \sqrt{(b^2 - ac)^2 + c^2 d^2}. \quad (22)$$

So the concurrence of the output state will be given by

$$C(\rho) = \max\{|\sqrt{\lambda_3} - \sqrt{\lambda_4}|, 0\}. \quad (23)$$

It is obvious that the concurrence depends on the parameters A , B , C , D . Since A and C can be given as functions of B due to Eqs. (10,11), $C(\rho)$ also depends on B . Unfortunately, the relation between $C(\rho)$ and B is too complicated to give in an explicit form, we will have to consider it in a numerical way.

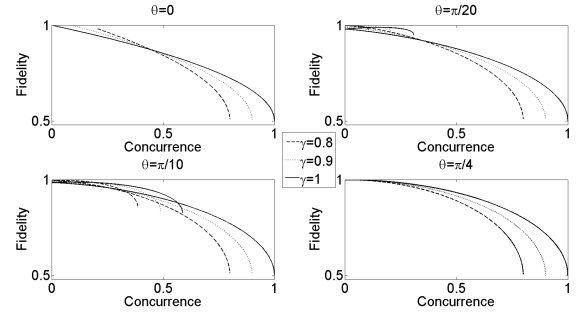


Fig. 1. The partially optimal fidelity f_p versus the concurrence. θ takes $0, \pi/20, \pi/10, \pi/4$ for each subplot, respectively, and $\gamma = 1, 0.9, 0.8$ for different line styles.

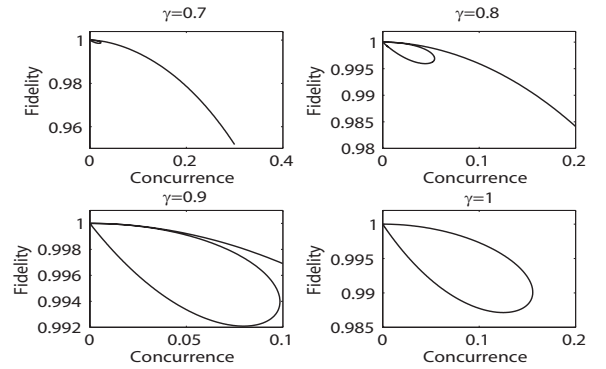


Fig. 2. The optimal fidelity $f_{(opt)}$ versus the concurrence with γ takes $0.7, 0.8, 0.9, 1$, respectively.

In principle, one can grasp any relation between the fidelity and the concurrence that depend on the common parameter B . In Fig.1, we plot how the partially optimal fidelity f_p in Eqs. (12,13) varies with the concurrence when the parameter θ of the input state is chosen as $0, \pi/20, \pi/10, \pi/4$ for different γ . From this figure, one could say that the large concurrence will lead to the decay of the fidelity for $\theta = 0$, however, for the other values of θ , there does not exist a one-to-one map between concurrence and the fidelity. It is obvious that the fidelity f_p could keep invariant, go up or go down for two different concurrence. In particular, this not only depends on the overlap between the two cloned states, but also depends on the probability. This can be seen from Fig. 1. It is interesting that, with the increase of θ , one can find that the single curve (for $\theta = 0$) will split into two curves with the same left end point. In particular, when $\theta = \pi/4$, the two curves almost coincide (we have carefully calculate the two curves that are too close to show explicitly in the figure). In addition, for different γ , the figures are similar, but the most obvious feature is that the small γ will limit the maximal concurrence that could be produced in the cloning. Therefore, for the general case, our conclusion is that the entanglement can not uniquely determine of the general fidelity.

In the following, we will discuss the relation between quantum entanglement and the optimal fidelity for the

unified $1 \rightarrow 2$ quantum cloning. From the partially optimal fidelity (12) and (13). Using the method of Lagrange multipliers, it is easy to derive an explicit expression from $\frac{\partial f_i(B)}{\partial B} = 0$. The reasonable value of parameter B reads

$$B_1 = \frac{s^2 - 1 + M}{8(s + s^2)}. \quad (24)$$

and

$$B_2 = -\frac{s^2 - 1 + M}{8(s + s^2)}. \quad (25)$$

with $M = \sqrt{1 + s^2[9s^2 + 16(1 + s)\gamma - 10]}$. Thus, replacing the B with (24) and (25) in Eqs. (12,13), respectively, the above two partially optimal fidelities will arrive at a common thoroughly optimal fidelity

$$f_{(opt)} = \frac{1}{2} + \frac{(3 + M - 3s^2)}{32\gamma} \sqrt{\frac{[2(s - 1)(1 - M + 3s^2) + 16s^2\gamma]}{s^2(1 + s)}} \quad (26)$$

In Fig 2, the plots show that how the optimal fidelity $f_{(opt)}$ varies with the concurrence when the parameter γ takes 0.7, 0.8, 0.9, 1. It is clear that even though for some particular γ , the concurrence and the fidelity show the converse trends, in general, they are not the one-to-one correspondence between them. That is, a fixed fidelity or probability could corresponds to different concurrence. In other words, a fixed concurrence could be enough for some input states to realize the cloning with some expectations (such as the fidelities or probabilities), but it could not enough for other states to realize the cloning with the same expectations. Compared with Fig. 1, one will find that the optimal fidelity corresponds to the narrow range of concurrence (not more than 0.4).

3.2 Quantum discord

As an important quantum correlation beyond quantum entanglement, quantum discord has been thought to be another physical resource in some quantum information processing tasks [33]. Recently some results have proven that in some quantum cloning, quantum discord is always present [30]. Next, we will employ the original quantum discord as a quantum correlation measure to study the quantum correlation in the unified $1 \rightarrow 2$ quantum cloning. Quantum discord $Q(\rho_{AB})$ introduced by Ollivier and Zurek [34], Vedral *et. al.* [35], respectively, is defined based on the loss of the information induced by some optimal measurements on only one subsystem

$$Q(\rho_{AB}) = \min_{\Pi_i^B} S_{\{\Pi_i^B\}}(\rho_{A|B}) + S(\rho_B) - S(\rho_{AB}), \quad (27)$$

where $S(\cdot)$ represents the von Neumann entropy and

$$S_{\{\Pi_i^B\}}(\rho_{A|B}) = \sum_j q_j S(\rho_A^j), \quad (28)$$

with the post-measured state ρ_A^j given by

$$\rho_A^j = \frac{\text{Tr}_B[(I_A \otimes \Pi_j^B)\rho_{AB}(I_A \otimes \Pi_j^B)]}{\text{Tr}_{AB}[(I_A \otimes \Pi_j^B)\rho_{AB}(I_A \otimes \Pi_j^B)]}, \quad (29)$$

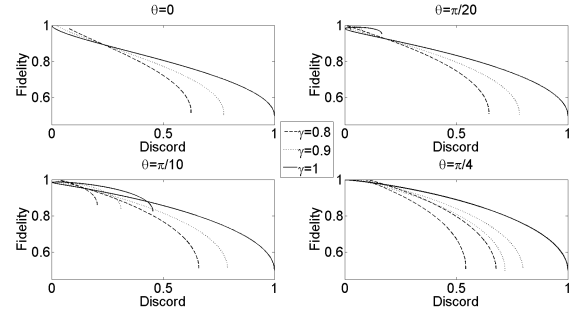


Fig. 3. The partially optimal fidelity f_p versus the quantum discord. θ takes $0, \pi/20, \pi/10, \pi/4$ for each subplot, respectively, and $\gamma = 1, 0.9, 0.8$ for different line styles.

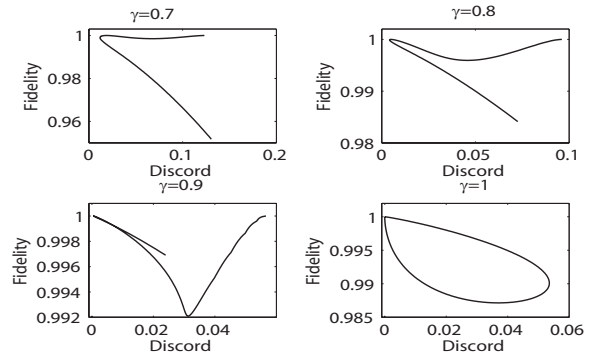


Fig. 4. The optimal fidelity $f_{(opt)}$ versus the quantum discord with γ takes 0.7, 0.8, 0.9, 1, respectively.

and q_j the corresponding probability given by

$$q_j = \text{Tr}_{AB}[(I_A \otimes \Pi_j^B)\rho_{AB}(I_A \otimes \Pi_j^B)]. \quad (30)$$

It is noted that $\{\Pi_j^B\}$ is a complete set of projective measurements.

Substitute Eq. (14) into Eq. (27), we can obtain the relation between the fidelity and the quantum discord. However, it is unfortunate that quantum discord given in Eq. (27) has not an analytic form for a general quantum state. So we have to numerically calculate the discord. In Fig. 3, it shows that how the partially optimal fidelity f_p in Eqs. (12,13) varies with the quantum discord and the input state with the parameter θ chosen as $0, \pi/20, \pi/10, \pi/4$ for $\gamma = 0.8, 0.9, 1$. From this figure, we also learn that the partially optimal fidelity and the quantum discord do not have a one-to-one correspondence. This is much like Fig. 1. However, one can note that when $\theta = \pi/4$, the two curves for $\gamma = 0.8, 0.9$ are separated clearly. While in Fig. 4, it shows that how the optimal fidelity $f_{(opt)}$ varies with quantum discord when the parameter γ takes 0.7, 0.8, 0.9, 1. From these figures, we can see that the quantum discord is not the unique factor that influences the fidelity of the unified $1 \rightarrow 2$ quantum cloning.

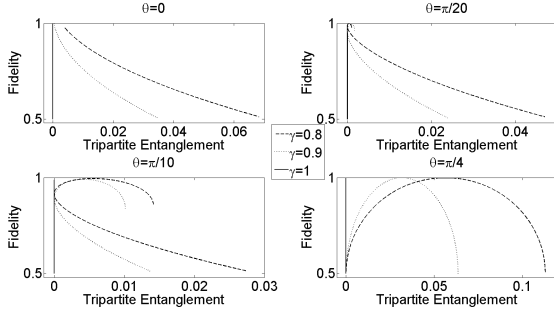


Fig. 5. The partially optimal fidelity f_p versus the tripartite entanglement (3-tangle τ). θ takes $0, \pi/20, \pi/10, \pi/4$ for each subplot, respectively, and $\gamma = 1, 0.9, 0.8$ for different line styles.

3.3 3-tangle

We've studied the bipartite correlation of the two output modes in the quantum cloning machine. The result shows that quantum correlation mainly depends on the quantum cloning scheme and the cloned states. However, the whole cloning procedure includes three parties. So, we would like to study the role of tripartite entanglement in the cloning machine. For a pure state $|\psi\rangle_{ABC}$ of three qubits, the 3-tangle $\tau(|\psi\rangle_{ABC})$ is a good entanglement measure which can be given by [35,36]

$$\tau(|\psi\rangle_{ABC}) = \sqrt{[Tr(\rho_{AB}\tilde{\rho}_{AB})]^2 - Tr[\rho_{AB}\tilde{\rho}_{AB}]^2}, \quad (31)$$

where $\tilde{\rho}_{AB} = \sigma_y \otimes \sigma_y \rho_{AB}^* \sigma_y \otimes \sigma_y$ with ρ_{AB} the reduced density matrix by tracing over party C . Thus substitute Eqs. (10), (11) and (14) into Eq. (31), one will find that the 3-tangle will arrives at

$$\tau(\rho_{ABC}) = \frac{(1-\gamma)}{\sqrt{2}} \left[\gamma - 2B^2(1 + \sin 2\theta) - \cos 2\theta \sqrt{1 - 4B^2 - \frac{2(1-\gamma)}{1 + \sin 2\theta}} \right]. \quad (32)$$

In particular, one will easily check that Eq. (10) and Eq. (11) will lead to the same result, i.e., Eq. (32). Thus for any $\gamma \geq \frac{1-s}{2}$, there always exists B that can connect the 3-tangle with the partially optimal fidelity f_p . Analogously, for the optimal cloning, the optimal fidelity $f_{(opt)}$ can also be related with the 3-tangle by s . We have illustrated the relations between the partially optimal fidelity f_p as well as the optimal fidelity $f_{(opt)}$ and the 3-tangle in Fig. 5. and Fig. 6. From the two figures, it is found that the 3-tangle vanishes when $\gamma = 1$ (the vertical line in the figures), which can be easily understood since $\gamma = 1$ corresponds to a product output state. One can easily find that these relations are analogous to those for bipartite entanglement. That is, the same 3-tangle could corresponds to different fidelities or probabilities.

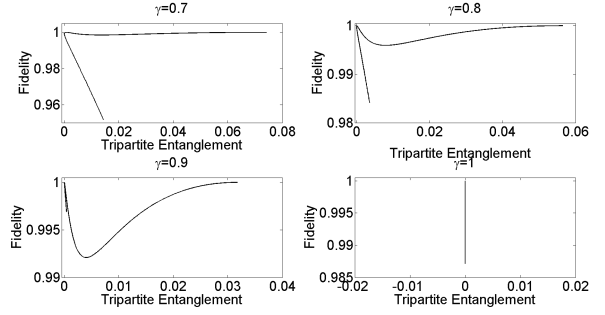


Fig. 6. The optimal fidelity $f_{(opt)}$ versus the tripartite entanglement (3-tangle τ) with γ takes 0.7, 0.8, 0.9, 1, respectively

4 Without any quantum correlation

From the above discussions, one can see that there is not a one-to-one relation between the fidelity and the various quantum correlations. The remaining question is whether quantum correlation is necessary for a successful quantum cloning. It is interesting that, in the unified $1 \rightarrow 2$ quantum cloning, quantum discord is actually not necessary at all. Let us choose some special constraint conditions on the reduced density matrix in the Eq. (14) as follows.

$$\gamma = 1 \quad (33)$$

$$b^2 = ac. \quad (34)$$

Thus, the reasonable values of parameters A and C can be given by

$$\begin{cases} A'_1 = \frac{1+s+\sqrt{(1+s)}}{2+2s}, \\ B'_1 = \frac{\sqrt{s}}{2\sqrt{1+s}}, \\ C'_1 = \frac{\sqrt{(1+s)}-(1+s)}{2+2s}. \end{cases} \quad (35)$$

$$\begin{cases} A'_2 = -\frac{1+s+\sqrt{(1+s)}}{2+2s}, \\ B'_2 = -\frac{\sqrt{s}}{2\sqrt{1+s}}, \\ C'_2 = \frac{(1+s)-\sqrt{(1+s)}}{2+2s}. \end{cases} \quad (36)$$

Thus, the state of the two output modes will be reduced to

$$Tr_p |\chi_1\rangle^{(out)} \langle \chi_1| = |\widetilde{\chi}_1\rangle \langle \widetilde{\chi}_1| \otimes |\widetilde{\chi}_1\rangle \langle \widetilde{\chi}_1|. \quad (37)$$

with $|\widetilde{\chi}_1\rangle = (\sqrt{a}|0\rangle \pm \sqrt{c}|1\rangle)$. It is obvious that the two output modes do not have either the quantum entanglement or quantum discord. Insert the Eqs. (35, 36) into Eq. (9), we will find that the cloning fidelity reads

$$f_{(no)} = \frac{1}{2} \left[1 + s^{\frac{3}{2}} + (1-s)\sqrt{1+s} \right]. \quad (38)$$

Although there is not any quantum correlation in the unified $1 \rightarrow 2$ quantum cloning, the quantum cloning machine that determined by the parameters Eqs. (35, 36) will still arrives at a large fidelity. One is able to find that the minimal value will achieve 0.9811 when the s is 0.3333. Finally, we would like to emphasize that even though there is no

quantum correlation in the cloning procedure, it is different from the classical cloning. The reason is that in the classical world, the overlap s for the two cloned states $|\chi_1\rangle$ and $|\chi_2\rangle$ must be $s = 0, 1$ which corresponds to the unit fidelity $f_{(no)}$, but it is not the case in the quantum world.

5 Discussions and Conclusion

We have studied the various quantum correlations including the concurrence, quantum discord and 3-tangle in the unified $1 \rightarrow 2$ state-dependent cloning and probabilistic quantum cloning. The results show that these quantum correlations in quantum cloning can not uniquely determine the characteristic parameters of the cloning such as the fidelity and success probability. These parameters depend on not only the various quantum correlations but also the quantum cloning scheme and the cloned states. In other words, for a fixed success probability or the fidelity, one could implement the quantum cloning with different quantum correlations. This could provide us a way to realize the quantum cloning with low cost (quantum correlations). In particular, we even find that the successful quantum cloning does not need any quantum correlation at all.

Finally, we would like to emphasize that all that we have studied are restricted to the case with real parameters A, B, C, D . It is natural that the case with the complex numbers will become quite complicated. However, we conjecture that the situation with complex parameters will lead to the analogous conclusion as our current results.

6 Acknowledgement

This work was supported by the National Natural Science Foundation of China, under Grants No.11375036 and 11175033.

References

1. C. H. Bennett, G. Brassard, C. Crpeau, R. Jozsa, A. Peres, W. K. Wootters, Phys. Rev. Lett. **70**, 1895 (1993).
2. C. H. Bennett, G. Brassard, S. Popescu, B. Schumacher, J. A. Smolin, W. K. Wootters, Phys. Rev. Lett. **76**, 722 (1996).
3. Z.-W. Wang, X.-F. Zhou, Y.-F. Huang, Y.-S. Zhang, X.-F. Ren, G.-C. Guo, Phys. Rev. Lett. **96**, 220505 (2006).
4. M. Koashi, N. Imoto, Phys. Rev. Lett. **77**, 2137 (1996).
5. C. H. Bennett, Phys. Rev. Lett. **68**, 3121 (1992).
6. V. Scarani, S. Iblisdir, and N. Gisin, Rev. Mod. Phys. **77**, 1225 (2005).
7. H. Fan, Y.-N. Wang, L. Jing, J.-D. Yue, H.-D. Shi, Y.-L. Zhang, and L.-Z. Mu, arXiv:1301.2956.
8. N. J. Cerf and J. Fiurasek, Progress in Optics **49**, 455 (2006).
9. W. K. Wootters, W. H. Zurek, Nature, **299**, 802 (1982).
10. L.-M. Duan, G.-C. Guo, Phys. Rev. Lett. **80**, 4999 (1998).
11. V. Bužek and M. Hillery, Phys. Rev. A **54**, 1844 (1996).
12. D. Bruß, D. P. DiVincenzo, A. Ekert, Phys. Rev. A **57**, 2368 (1998).
13. D. Bruß, M. Cinchetti, G. M. D'Ariano, and C. Macchiavello, Phys. Rev. A **62**, 012302 (2000).
14. C.-S. Niu, and R. B. Griffiths, Phys. Rev. A **60**, 2764 (1999).
15. N. Gisin and S. Massar, Phys. Rev. Lett. **79**, 2153 (1997).
16. H. Fan, K. Matsumoto, X.-B. Wang, and M. Wadati, Phys. Rev. A **65**, 012304 (2001).
17. G. M. D'Ariano and C. Macchiavello, Phys. Rev. A **67**, 042306 (2003).
18. G. M. D'Ariano and P. Lo Presti, Phys. Rev. A **64**, 042308 (2001).
19. H. Fan, H. Imai, K. Matsumoto, and X.-B. Wang, Phys. Rev. A **67**, 022317 (2003).
20. K. Bartkiewicz and A. Miranowicz, Phys. Rev. A **82**, 042330 (2010).
21. F. Anselmi, A. Chefles, and M. B. Plenio, New J. Phys. **6**, 164 (2004).
22. V. Bužek, V. Vedral, M. B. Plenio, P. L. Knight, and M. Hillery, Phys. Rev. A **55**, 3327 (1997).
23. S. Ghosh, G. Kar, and A. Roy, Phys. Rev. A **69**, 052312 (2004).
24. M. Owari and M. Hayashi, Phys. Rev. A **74**, 032108 (2006).
25. J. Fiurásek, S. Iblisdir, S. Massar, and N. J. Cerf, Phys. Rev. A **65**, 040302 (2002).
26. W.-H. Zhang, L.-B. Yu, Z.-L. Cao, and L. Ye, Phys. Rev. A **86**, 022322 (2012).
27. Y.-N. Wang, H.-D. Shi, Z.-X. Xiong, L. Jing, X.-J. Ren, L.-Z. Mu, and H. Fan, Phys. Rev. A **84**, 034302 (2011).
28. V. Bužek, M. Hillery, Phys. Rev. A **54**, 1844 (1996).
29. S. Sazim, I. Chakrabarty, A. Datta, and A. K. Pati, arXiv:1308.4340.
30. L. Roa, M. Alid-Vaccarezza, C. Jara-Figueroa and A. B. Klimov, Phys. Lett. A, **378** 941-945 (2014).
31. T. Durt and J. Van de Putte, Int. J. Quant. Inform. **9**, No. 3, 915-936 (2011).
32. W. K. Wootters, Phys. Rev. Lett. **80**, 2245 (1998).
33. K. Modi, A. Brodutch, H. Cable, T. Paterek and V. Vedral, Rev. Mod. Phys. **84**, 1655 (2012).
34. H. Ollivier and W. H. Zurek, Phys. Rev. Lett. **88**, 017901 (2001).
35. L. Henderson, and V. Vedral, J. Phys. A: Math. Theor. **34**, 6899 (2001).
36. V. Coffman, J. Kundu, and W. K. Wootters, Phys. Rev. A **61**, 052306 (2000).
37. C.-S. Yu, H.-S. Song and Y.-H. Wang, Quant. Inf. Comp. **7**, 584 (2007).